Uncertainty estimates for the LA19-13-03 VNA

Nils Nazoa
LA Techniques Ltd
August 2013

CONTENTS

1 Introduction

This document provides uncertainty estimates for reflection and transmission measurements made using the LA19-13-03 Vector Network Analyser (VNA) in conjunction with LA Techniques' 3.5 mm calibration kits that use loads characterised using the method described in [1]. This characterisation process provides increased measurement accuracy for a VNA calibrated using kits containing such loads.

The methods used to evaluate the uncertainty in the VNA follow recognised practices [3]; these being based on internationally agreed guidelines [4]. The uncertainty estimates do not include contributions due to random errors (e.g. connector repeatability, system repeatability, cable flexure, noise and ambient conditions).[1] These estimates therefore provide a Best Measurement Capability [5] suitable for defining a Scope of Accreditation [6] for measurements made using this type of VNA and calibration kit. [2]

The following are the conditions used to obtain results for this report.

Instrument Test Conditions:

Test signal level:	+3 dBm
Number of sweep points:	201
Measurement bandwidth:	20Hz
Averaging:	16
Port 1 calibration kit:	LA Techniques DW97046 (male kit)
Port 2 calibration kit:	LA Techniques DW97045 (female kit)
Evaluation frequency range:	1MHz to 8GHz

In section 2, the size of each of the six uncertainty contributions considered in this document is evaluated. For convenience, the resulting values established for these uncertainty contributions are summarised in Tables 1 and 2, below. Section 3 presents the methods used to express uncertainty, including the use of logarithmic quantities (specifically, return loss) and phase. Sections 4 and 5 present overall uncertainty estimates for reflection and transmission measurements, respectively, and Section 6 presents some example results and comparisons with measurements taken using an Anritsu 36379C instrument, calibrated employing an Agilent 8533E 3.5mm calibration kit.

[1] Except for noise, these random errors come from 'outside' the VNA and so are not representative of the VNA's performance. They are caused by the other components involved in the overall measurement process – i.e. the cables and adaptors used to form the test port reference planes, the devices connected to the reference planes (both calibration standards and devices under test) – and the environment in which the VNA is operated.

[2] However, since worst-case estimates are used in this document to represent each of the uncertainty components that are considered, the resulting overall uncertainty estimates may well be comparable with user uncertainty estimates that may need also to take into account the random error effects – i.e., assuming that these random errors are not the dominant errors in the measurements.

Table 1: Uncertainty contributions for reflection measurements (linear units)

Directivity	Test Port Match	Load Match
0.003	0.005	0.005

Table 2: Uncertainty contributions for transmission (attenuation) measurements

Non-linearity	Isolation/cross/talk	Mismatch
0.0015 dB/dB	-103 dB	0.014 dB

2 Uncertainty contributions

2.1 Residual directivity

The residual directivity of the calibrated VNA is assessed by attaching a beadless air line terminated with a well-matched load to each of the VNA's test port reference planes. The traces obtained, presented in terms of linear voltage reflection coefficient (VRC), are shown in Figure 1. The residual directivity is given by half the difference between adjacent maxima and minima of the observed ripple trace [3].

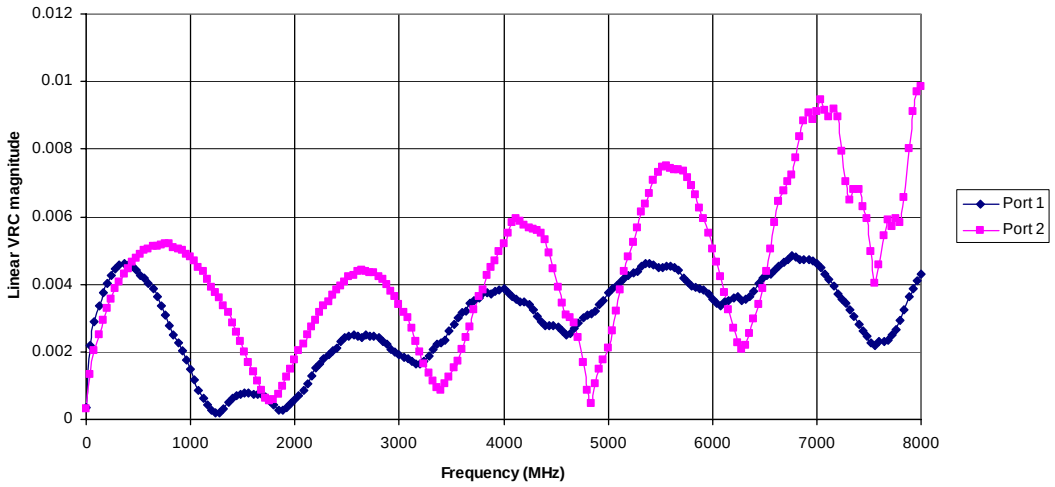

Figure 1: Ripple trace due to residual directivity in the calibrated VNA

The worst-case observed value for the residual directivity, D, after allowing for the slope of the trace is therefore:

$$D = \frac{(0.008 - 0.0002)}{2} \approx 0.003 \equiv -50 \text{ dB}$$

2.2 Residual test port match

The residual test port match of the calibrated VNA is assessed by attaching a beadless air line terminated with a high reflect (e.g. a short-circuit) to each of the VNA's test port reference planes. The traces obtained (in terms of VRC) are shown in Figure 2. The residual test port match is given by half the difference between the adjacent maxima and minima of the observed ripple trace [3].

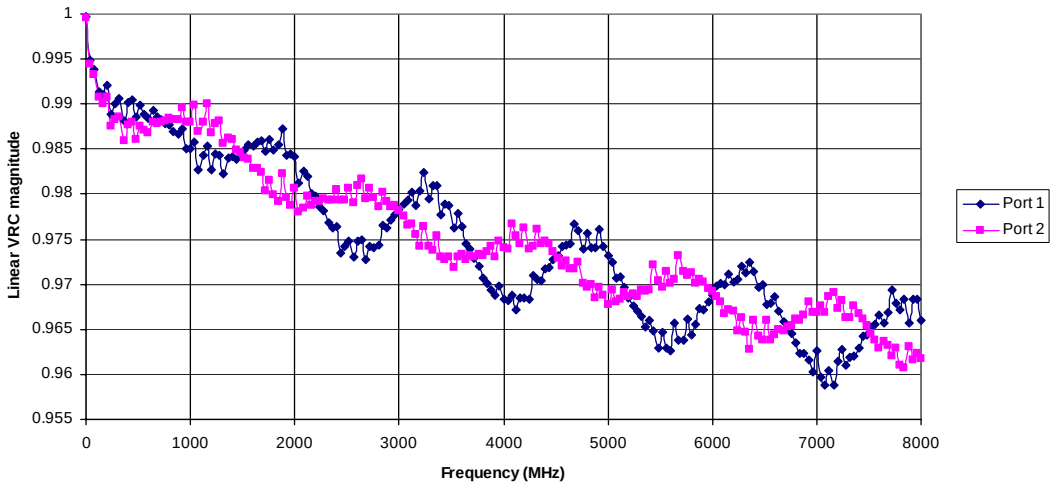

Figure 2: Ripple trace due to residual test port match in the calibrated VNA

The worst-case observed value for the residual test port match, *M*, after allowing for the slope of the trace is therefore:

$$M = \frac{(0.97 - 0.96)}{2} \approx 0.005 \equiv -46 \text{ dB}$$

2.3 Residual load match

The residual load match, Γ_L, is related to the uncertainty in measuring the reflection coefficient of the actual (uncorrected) load match, Γ, of the VNA's receiver port. (The receiver port will be port 2 when measuring in the forward direction and port 1 when measuring in the reverse direction.) Therefore, the residual load match can be estimated using [3]:

$$\Gamma_L = 2\left(\frac{D}{\sqrt{2}} + \frac{M\Gamma^2}{\sqrt{2}}\right) \quad (1)$$

A measurement of the uncorrected load match, Γ, is shown in Figure 3. This shows that Γ for both ports is less than 0.29 and so the worst-case observed value for Γ_L is given as:

$$\Gamma_L = 2\left(\frac{0.003}{\sqrt{2}} + \frac{0.005 \times 0.29^2}{\sqrt{2}}\right) \approx 0.005 \equiv -46 \text{ dB}$$

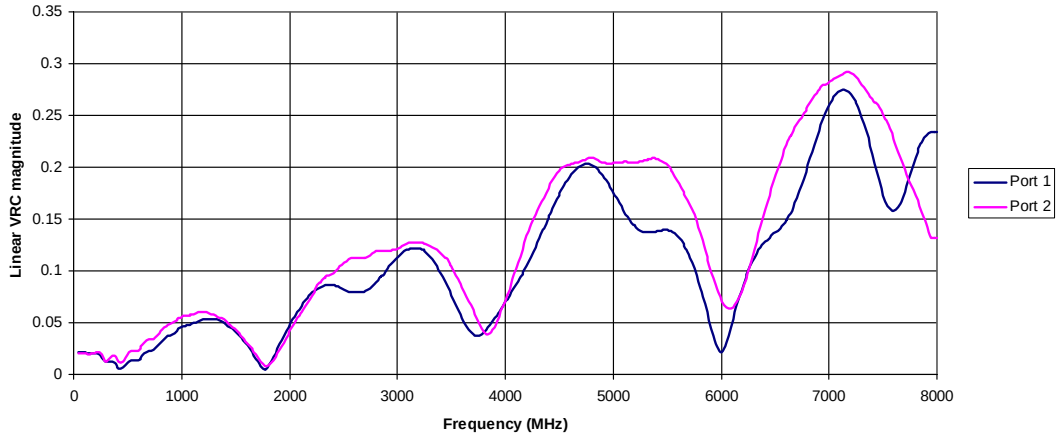

Figure 3: Measured uncorrected load match at ports 1 and 2

2.4 Non-linearity

The non-linearity in the VNA's transmission measurements is assessed by measuring a calibrated step attenuator at one or more frequencies across the VNA's bandwidth. On this occasion, an assessment of non-linearity was made at a relatively low frequency (50 MHz) and a relatively high frequency (1000 MHz) within the VNA's bandwidth.

The procedure [3] for determining non-linearity uses results obtained over a 10 dB to 50 dB range, in steps of 5 dB. At each value of attenuation, the attenuation measured by the VNA is compared with the calibrated value. The difference between these values divided by the nominal attenuation value is referred to as the VNA's non-linearity. Figures 4 and 5 show the results obtained at 50 MHz and 1000 MHz, respectively.

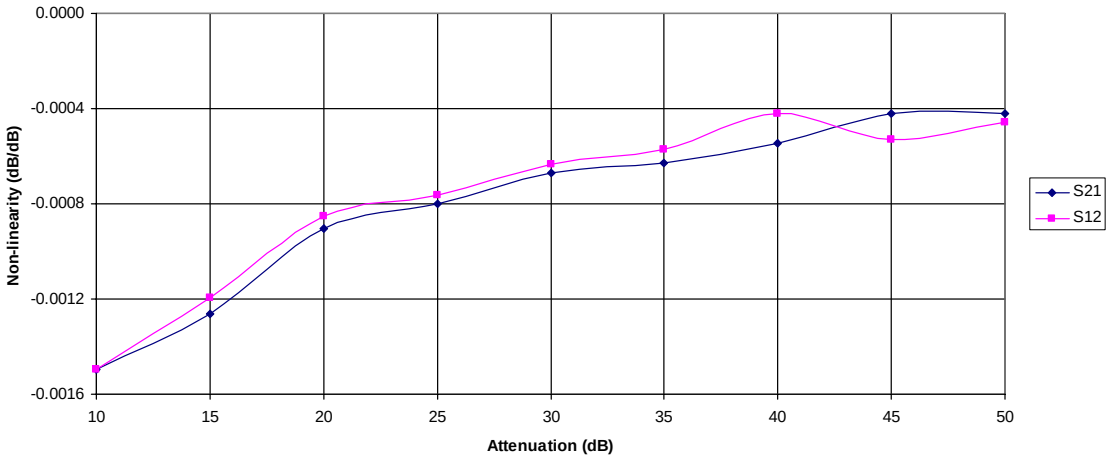

Figure 4: Measured non-linearity at 50 MHz

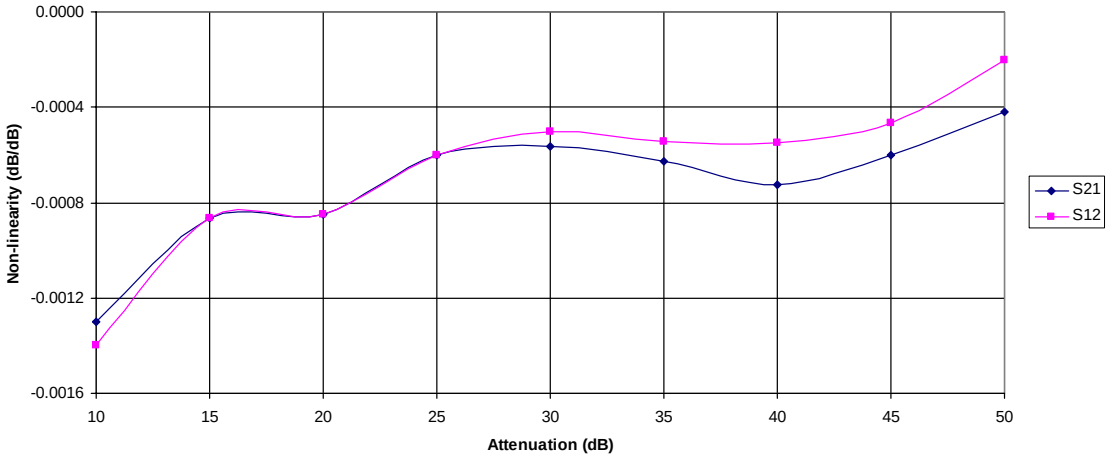

Figure 5: Measured non-linearity at 1000 MHz

These plots are further summarized in Table 3, in terms of the maximum observed non-linearity at all measured levels of attenuation. Based on these values, a worst-case value of 0.0015 dB/dB is used to represent the uncertainty contribution due to VNA non-linearity at all measurement frequencies.

Table 3: Summary of measured non-linearity at 50 MHz and 1000 MHz

Frequency	**Maximum observed non-linearity (dB/dB)**	
	S_{21}	S_{12}
50 MHz	0.001 5	0.001 5
1000 MHz	0.001 3	0.001 4

2.5 Isolation/cross-talk

The isolation/cross-talk in the VNA is determined by measuring (as S_{21} and S_{12}) the amount of signal that is transmitted and detected when both ports of the VNA are terminated with one-port devices. On this occasion, the one-port devices were chosen to be matched loads. The observed transmission responses are shown in Figure 6, along with two straight lines that have been fitted to each plot.

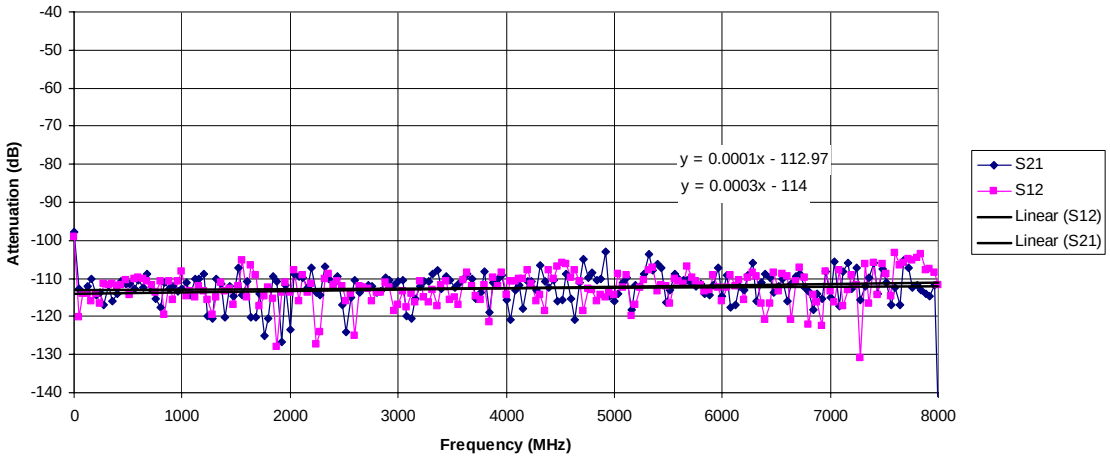

Figure 6: Measured isolation using a test level of +3 dBm

The equations to these straight lines are used to show the average variation in isolation/cross-talk as a function of frequency. This information is further summarised in Table 4, along with the worst-case value (-103 dB) that is used to represent the isolation/cross-talk uncertainty contribution, *I*, for the VNA.

Table 4: Summary of measured isolation (F>1MHz)

S-parameter	Isolation/cross-talk at 10 MHz	Isolation/cross-talk at 8 GHz	Worst case isolation/cross-talk
S_{21}	-113 dB	-112 dB	-103 dB
S_{12}	-114 dB	-113 dB	-103 dB

During measurement of a particular device under test, the size of the uncertainty contribution due to isolation/cross-talk, *dA*, will vary depending on the measured attenuation, *A*, according to [3]:[3]

$$dA = 20\log_{10}\left[1+10^{\frac{(I+A)}{20}}\right] \qquad (2)$$

This is shown in Figure 7, for measured attenuation ranging from 0 dB to 100 dB.

[3] This equation has been modified to take account of the negative sign used here for the isolation term, i.e. I = -103 dB rather than I = +103 dB, as would be used in [3]. This also assumes that the measured attenuation, A, is expressed as a positive number, e.g. A = +20 dB.

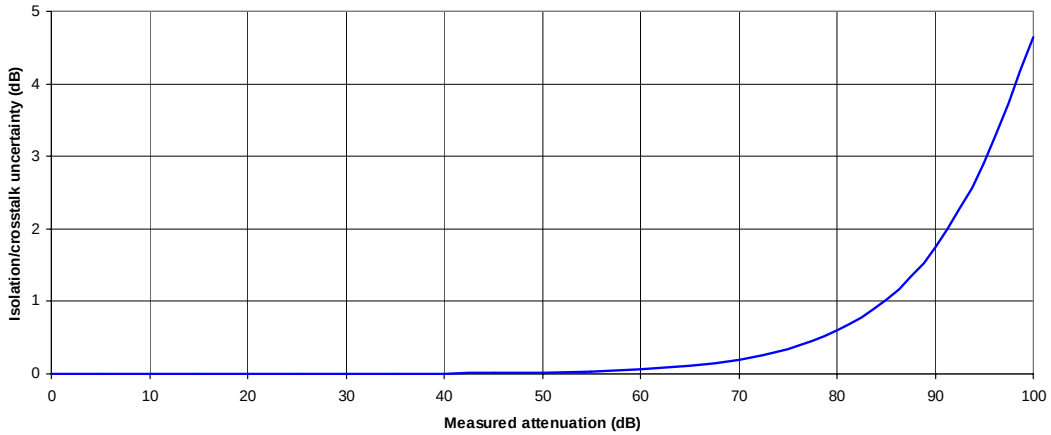

Figure 7: Isolation/cross-talk uncertainty contribution

2.6 Mismatch

The expression used to evaluate the mismatch uncertainty contribution is [3]:

$$M_{\mathrm{TM}} = 20\log_{10}\frac{1+(|MS_{11}|+|\Gamma_L S_{22}|+|M\Gamma_L S_{11}S_{22}|+|M\Gamma_L S_{21}S_{12}|)}{1-|M||\Gamma_L|} \qquad (3)$$

Only relatively well-matched devices (where S_{11} and S_{22} will not be greater than 0.15) are considered here. Therefore, for uncertainty budgeting purposes, it is assumed that $S_{11} = S_{22} = 0.15$.[4] Under these conditions, the worst-case value of M_{TM} is 0.014 dB (regardless of the values of S_{21} and S_{12}).

3 Expressing uncertainty

3.1 Expanded uncertainty

In the sections that follow, the overall uncertainties quoted for both reflection and transmission measurements are expanded uncertainties [4] that define an interval estimated to have a level of confidence of 95 percent. This is common practice for expressing uncertainties for measurements at RF and microwave frequencies.

3.2 Uncertainty expressed in dB

For reflection measurements, uncertainty is evaluated in terms of VRC (i.e. S_{11} and S_{22}) then converted to the equivalent return loss uncertainty, $U(RL)$, using [7]:

[4] For devices where S_{11} and S_{22} are greater than 0.1, these calculations need to be repeated using the measured values of S_{11} and S_{22} in the above equation.

$$U(RL) \approx 8.686 \times \frac{U(|S_{ii}|)}{|S_{ii}|} \tag{4}$$

where S_{ii} (i = 1, 2) is the measured reflection coefficient and $U(|S_{ii}|)$ is the expanded uncertainty in $|S_{ii}|$.

3.3 Uncertainty in phase

For a given S-parameter, S_{ij} (i = 1, 2; j = 1, 2), the expanded uncertainty in phase, $U(\varphi)$, can be estimated using [8]:

$$U(\varphi) = \sin^{-1}\left(\frac{U(|S_{ij}|)}{|S_{ij}|}\right) \tag{5}$$

where S_{ij} is the measured S-parameter and $U(|S_{ij}|)$ is the expanded uncertainty in $|S_{ij}|$.

When calculating the uncertainty in transmission phase, it is first necessary to determine the uncertainty in the magnitude of the linear transmission coefficient (i.e. $U(|S_{21}|)$ or $U(|S_{12}|)$). This can be derived from the measured attenuation, A, and the uncertainty in the measured attenuation, $U(A)$ using [7]:

$$U(|S_{ij}|) \approx \frac{1}{8.686} \times 10^{-\frac{A}{20}} \times U(A) \tag{6}$$

4 Uncertainty in reflection measurements

4.1 One-port devices

The uncertainty, $U(\Gamma)$, of a VRC measurement of a one-port device can be estimated using [3]:

$$U(\Gamma) = 2\left(\frac{D}{\sqrt{2}} + \frac{M\Gamma^2}{\sqrt{2}}\right) \tag{7}$$

where Γ is the measured VRC of the device under test. Using the values of D and M determined in section 2, a plot of the return loss uncertainty as a function of measured return loss is shown in Figure 8. The associated uncertainty in reflection phase is shown in Figure 9.

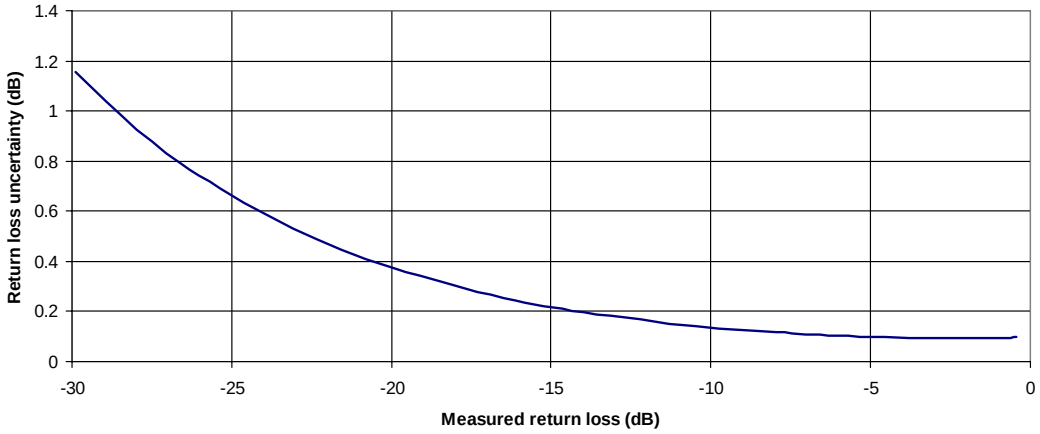

Figure 8: Return loss uncertainty for one-port devices

Figure 9: Reflection phase uncertainty for one-port devices

4.2 Two-port devices

The uncertainty, $U(\Gamma)$ of a VRC measurement of a two-port device can be estimated using [3]:

$$U(\Gamma) = 2\sqrt{\left(\frac{D}{\sqrt{2}} + \frac{M\,\Gamma^2}{\sqrt{2}}\right)^2 + \left(\frac{\Gamma_L {S_{21}}^2}{2}\right)^2} \qquad (8)$$

where Γ and S_{21} are the measured VRC and linear transmission coefficient, respectively, of the device under test. This is assumed to apply to both forward and reverse directions (i.e. for reciprocal devices having $S_{21} = S_{12}$). This expression is similar to the one used for one-port VRC measurements (equation (7)), and only becomes significantly different when measuring

low values of attenuation (i.e. when $S_{21} > 0.7$ or, equivalently, when the measured attenuation is less than 3 dB). Therefore, as a rule of thumb, when the measured attenuation is greater than 3 dB, the return loss and reflection phase uncertainty is that shown in Figures 8 and 9, respectively. When the measured attenuation is less than 3 dB, the return loss and reflection phase uncertainty is shown in Figures 10 and 11, respectively.

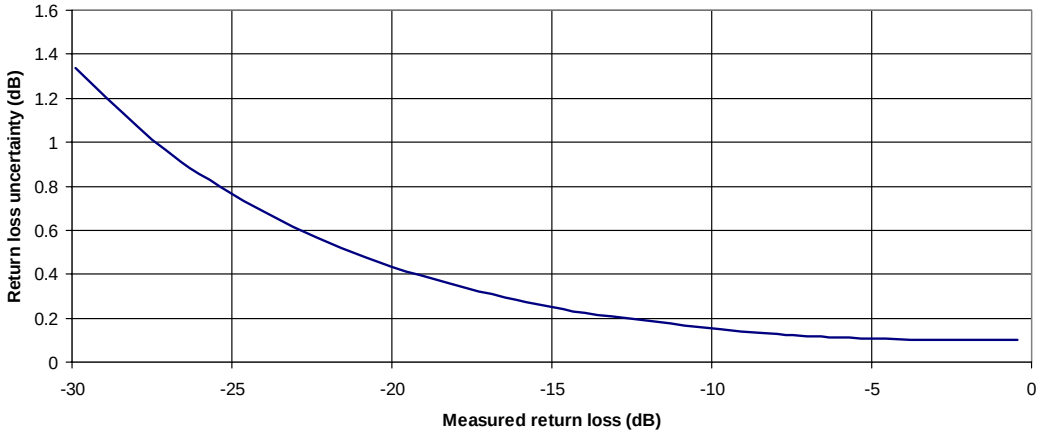

Figure 10: Return loss uncertainty for two-port devices with low attenuation (i.e. < 3 dB)

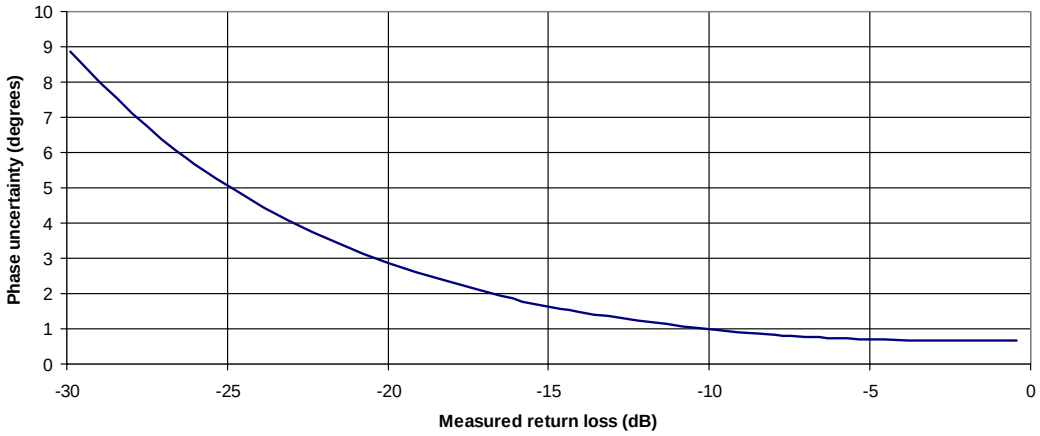

Figure 11: Reflection phase uncertainty for two-port devices with low attenuation (i.e. < 3 dB)

5 Uncertainty in attenuation/transmission coefficient measurements

The uncertainty, *U*, of an attenuation measurement of a two-port device can be estimated using [3]:

$$U = 2\sqrt{\left(\frac{L}{2}\right)^2 + \left(\frac{M_{TM}}{\sqrt{2}}\right)^2 + \left(\frac{dA}{\sqrt{3}}\right)^2} \tag{9}$$

Using the values of L, M_{TM} and dA determined in section 2, plots of the attenuation uncertainty are shown in Figure 12 (for measured attenuation from 0 dB to 70 dB) and Figure 13 (for measured attenuation from 40 dB to 90 dB). The respective uncertainty in transmission phase associated with these two ranges of attenuation is shown in Figures 14 and 15. The plots assume the DUT has S11 and S22 values of less than 0.15 (well matched). Also, the plots are adjusted to include the quadrature error of 0.01dB associated with the instrument's hardware.

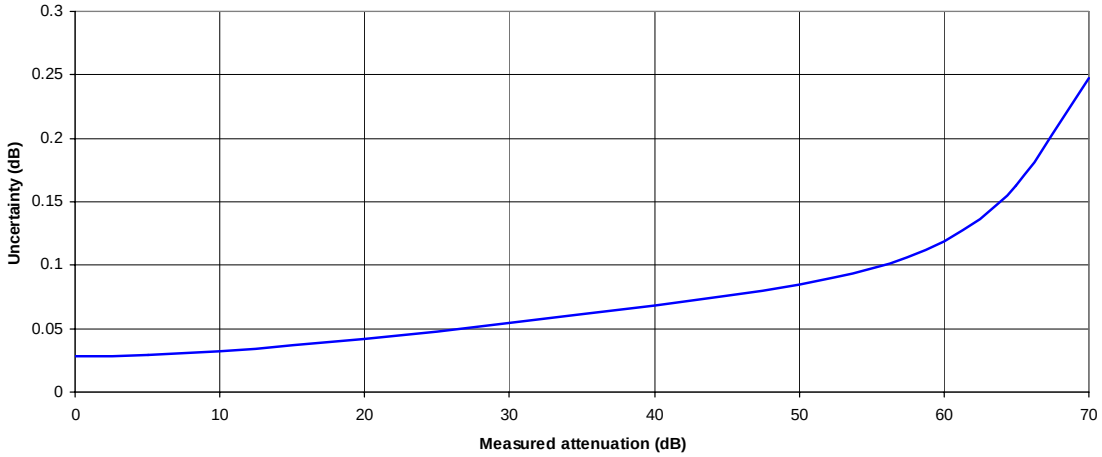

Figure 12: Attenuation uncertainty for measurements to 70 dB

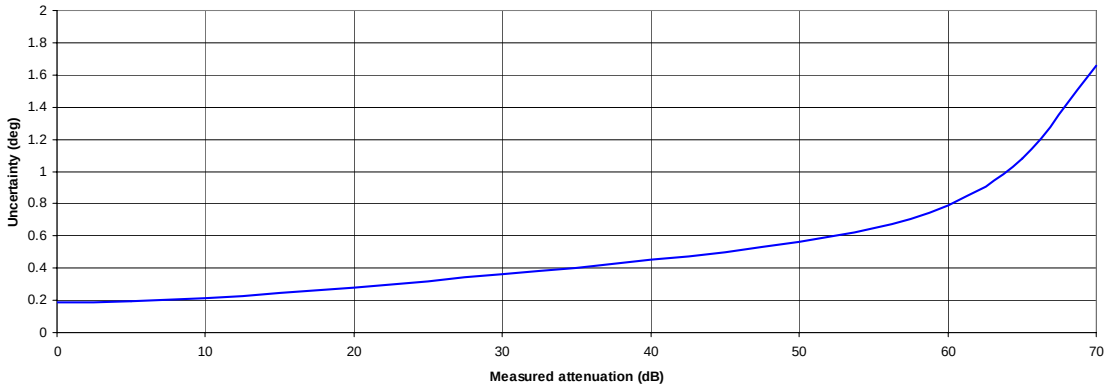

Figure 13: Attenuation phase uncertainty for measurements to 70 dB

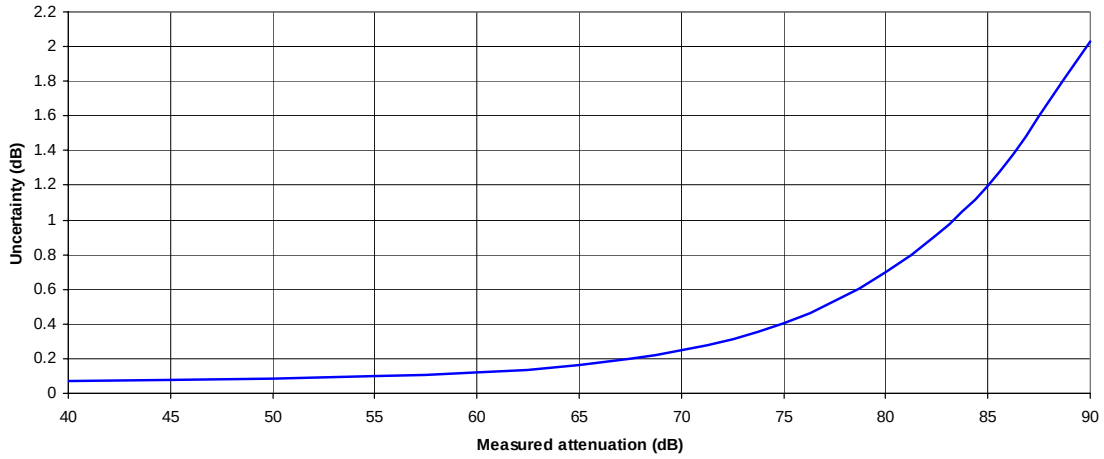

Figure 14: Transmission uncertainty for attenuation measurements above 40 dB

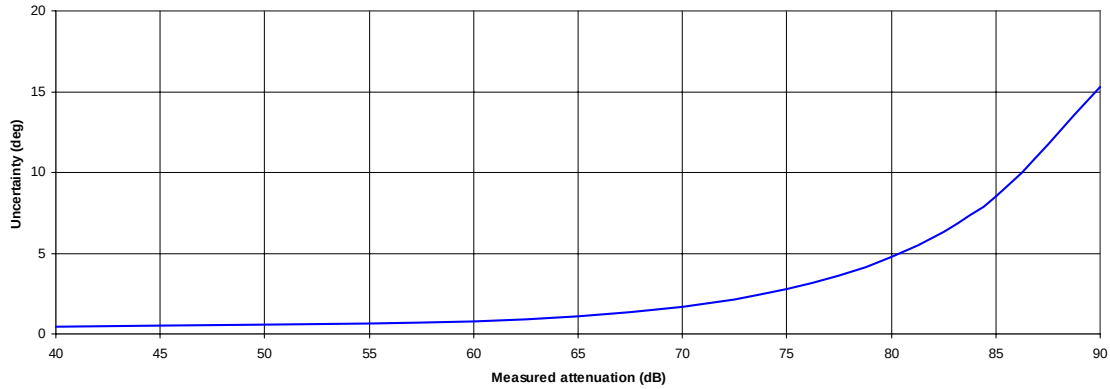

Figure 15: Transmission phase uncertainty for attenuation measurements above 40 dB

6 Examples and comparisons

This section presents comparisons of measurements made using the LA19-13-03 VNA (using the LA DW97045 and DW97046 3.5mm calibration kits) against measurements made using an Anritsu model 37369C calibrated using an Agilent 8533E 3.5mm calibration kit.

A plot of the difference between the measurements is shown for both phase and amplitude as a way of presenting the comparison. The maximum applicable uncertainty for the measurement, calculated in this document for the LA19-13-03, is marked on the plots. The uncertainty contribution by the Anritsu 37369C is ignored.

6.2 Beatty Line

6.2.1 Transmission measurement

A 150mm long Beatty mismatch line was measured. The measured transmission results are shown in Fig. 18a, 18b and 18c. Note that the reflection coefficient of the Beatty line reach up to 0.6 and therefore, larger (and variable) uncertainty values apply as shown in Fig. 16 of this document.

The graphs in Figs. 18b and 18c include uncertainty markers limits. These uncertainty values are derived as described in this document. No contribution from the Anritsu 37369C instrument is included for ease of comparison.

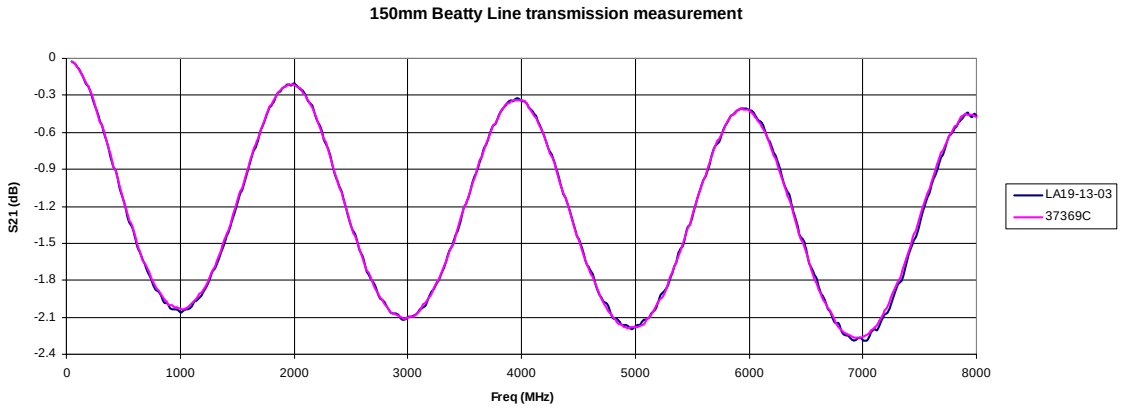

Figure 18a: Measurement comparison (between LA19-13-03 and Anritsu 37369C) for the forward transmission loss (S21) of a Beatty line.

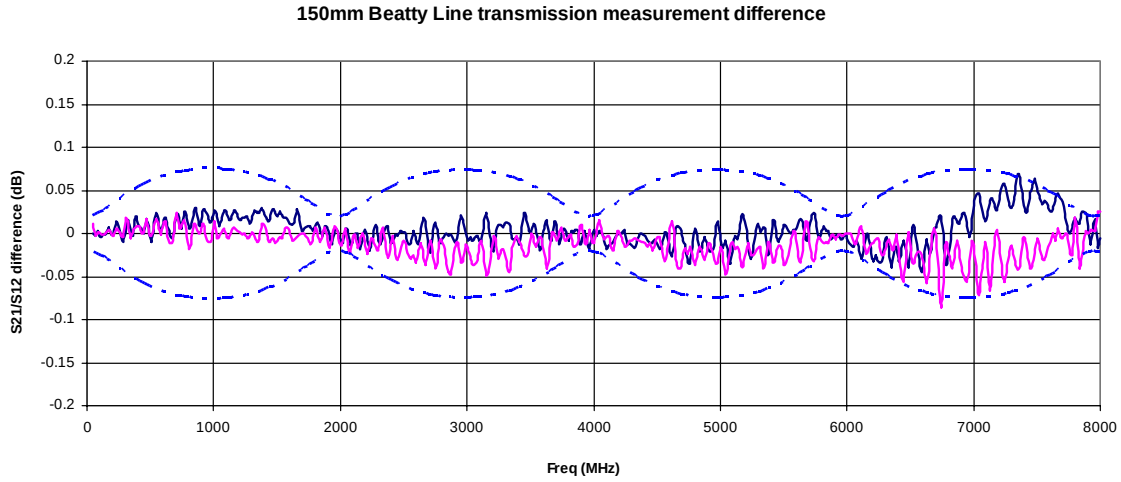

Figure 18b: Difference in the measurement of amplitude of S21 and S12 between LA19-13-03 and Anritsu 37369C for a Beatty line. Dotted lines are calculated (in this document) uncertainty limits for the LA19-13-03.

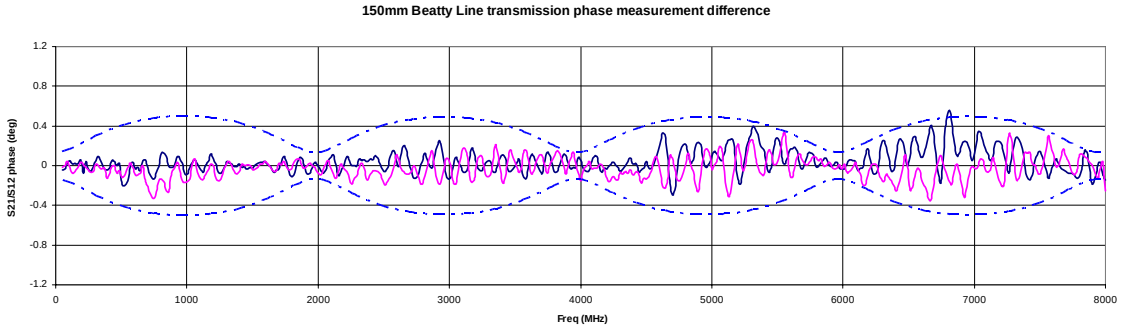

Figure 18c: Difference in the measurement of phase of S21 and S12 between LA19-13-03 and Anritsu 37369C of a Beatty line. Dotted lines are calculated uncertainty limits for the LA19-13-03.

6.2.2 Reflection measurement

Superimposed plots of measurements of the amplitude of S11 are shown in Fig. 19a. The difference between the two measurements for both S11 and S22 are plotted in Fig. 19b. This also includes the applicable uncertainty limits calculated for the LA19-13-03. As stated before, the uncertainty contribution made by the Anritsu 37369C was ignored.

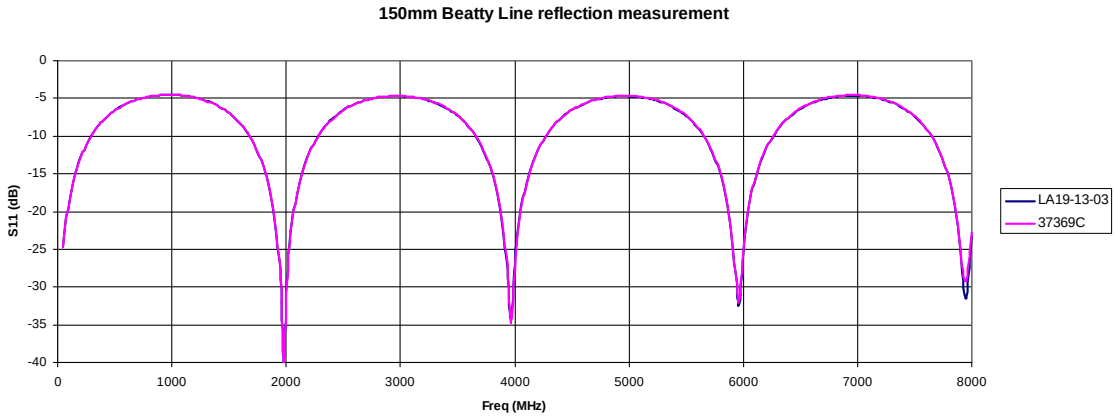

Figure 19a: Reflection measurement comparison of a Beatty line

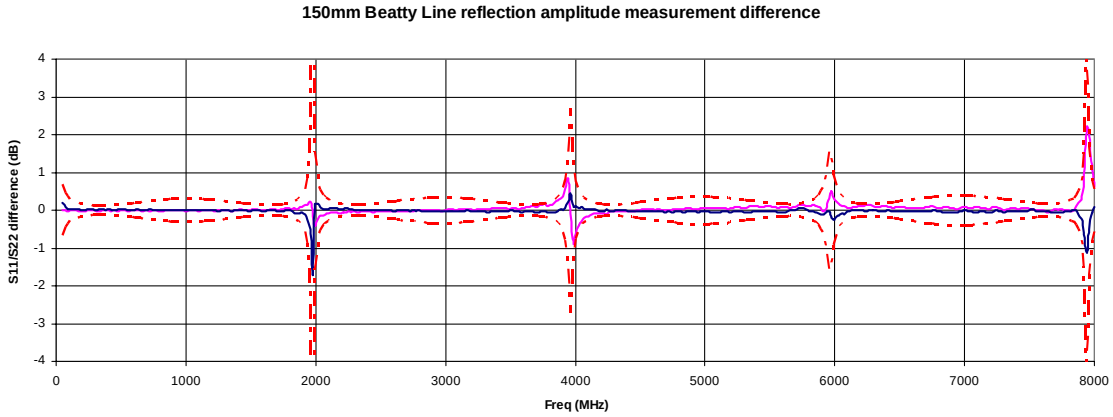

Figure 19b: Difference in the measurement of amplitude of S11 and S22 between LA19-13-03 and Anritsu 37369C of a Beatty line. Dotted lines are calculated (in this document) uncertainty limits for the LA19-13-03.

6.3 40 dB Attenuator

A coaxial attenuator was measured and the results compared in the same manner. Figure 20a shows the results for the forward transmission loss. It can be seen that, apart from a low frequency anomaly in the 37369C results, the measurements fall well within the uncertainty limits of the LA19-13-03 alone. Similar results were seen for the reverse transmission loss.

The difference in the phase measurements between the instruments is shown in Fig.20b. As for the amplitude results, apart from a low frequency anomaly in the 37369C results, the plot of the difference in phase falls within the uncertainty limits of the LA19-13-03 alone.

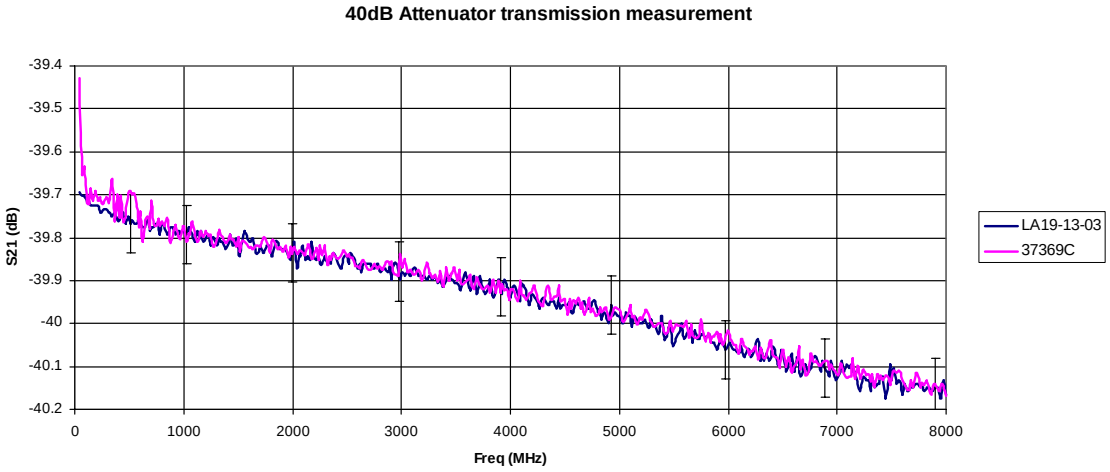

Figure 20a: Measurement comparison for the forward transmission loss (S21) of a 40 dB attenuator. The uncertainty bars represent the calculated uncertainty of the LA19-13-03. Contribution to uncertainty from all other sources was ignored.

`

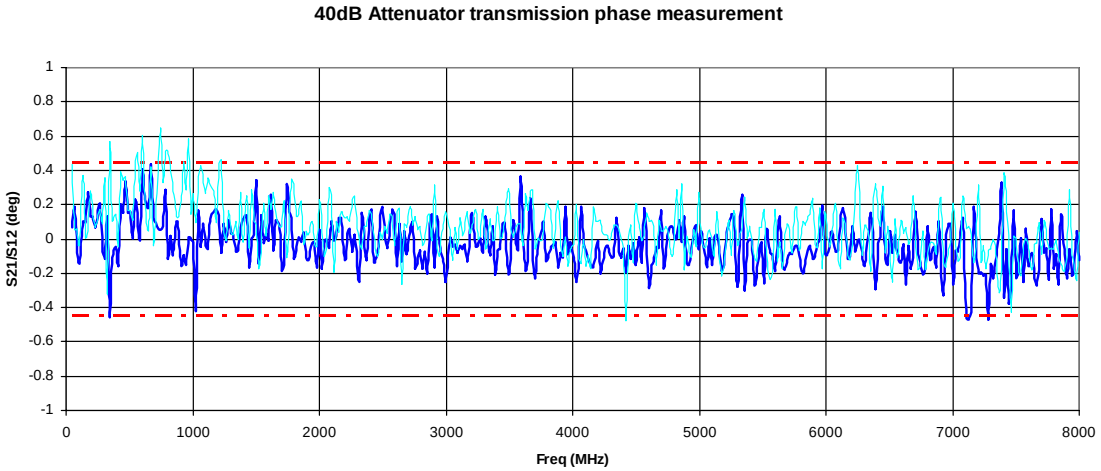

Figure 20b: Difference in the measurement of phase of S21 and S12 between LA19-13-03 and Anritsu 37369C of a 40dB attenuator. Dotted lines are calculated (in this document) LA19-13-03 uncertainty.

7 Observations and summary

The comparisons in section 6 show good agreement between the LA19-13-03 VNA measurements and the Anritsu 37369C reference values (i.e. the uncertainty intervals for nearly all the LA19-13-03 measurements encompass the reference values). This shows that the sizes of the uncertainty intervals established in this document are realistic – being neither optimistic (i.e. too small) nor pessimistic (i.e. too large).

8 References

[1] Nick Ridler and Nils Nazoa, "Using simple calibration load models to improve accuracy of vector network analyser measurements", *67th Automatic RF Techniques Group (ARFTG) conference digest*, pp 104-110, San Francisco, California, USA, June 2006.

[2] Nils Nazoa and Nick Ridler, "LA19-13-01 3 GHz VNA calibration and measurement uncertainty", *LA Techniques Ltd,* Technical Note Ref LAP02, January 2006. (Available from www.latechniques.com.)

[3] "EA guidelines on the evaluation of Vector Network Analysers (VNA)", *European co-operation for Accreditation*, publication reference EA-10/12, May 2000.

[4] "Guide to the expression of uncertainty in measurement", *International Organization for Standardization*, 1995.

[5] "Expression of the uncertainty of measurement in calibration", *European co-operation for Accreditation*, publication reference EA-4/02, December 1999.

[6] ISO/IEC 17025: 2005, "General requirements for the competence of testing and calibration laboratories".

[7] N M Ridler, "Converting between logarithmic and linear formats for reflection and transmission coefficients", ANAMET ANA_tips Technical Note No 4, October 2000. (Available from www.npl.co.uk/anamet.)

[8] N M Ridler and J C Medley, "An uncertainty budget for VHF and UHF reflectometers", *NPL Report DES 120*, May 1992. (Available from www.npl.co.uk.)

[9] "International vocabulary of basic and general terms in metrology", *International Organization for Standardization*, 2nd edition, 1993.